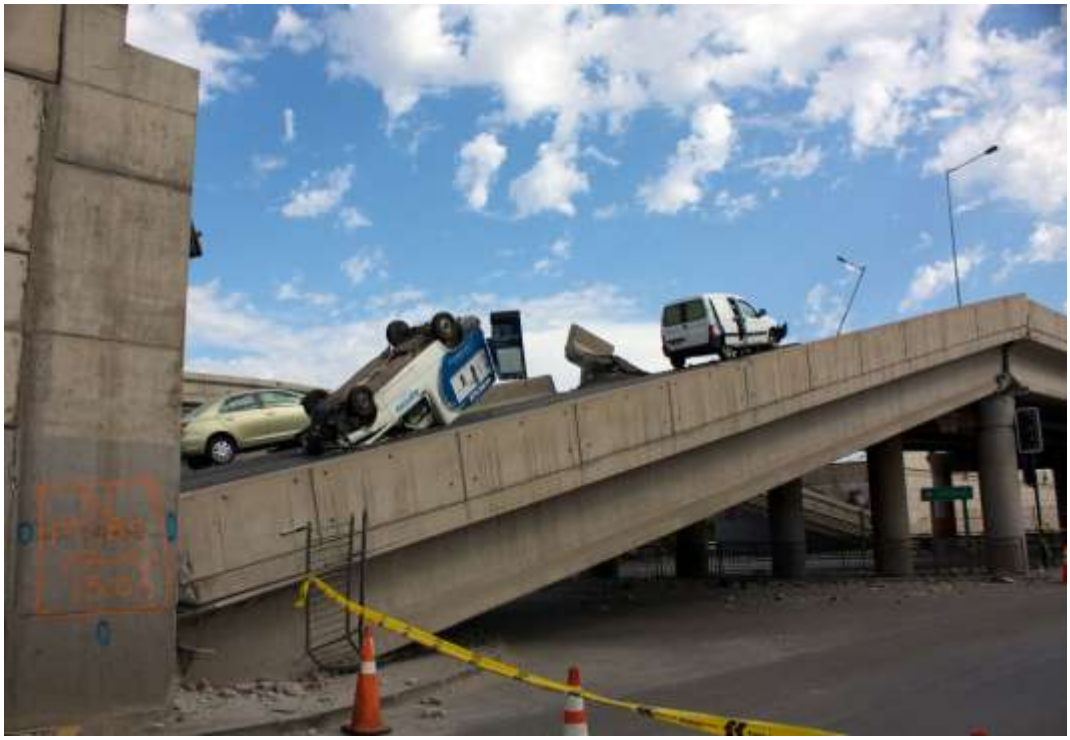

By Esteban Maldonado, Santiago, Chile. https://commons.wikimedia.org/w/index.php?curid=9670264

Fellenius, B.H., Abbasi, B., and Muhunthan, B., 2020. Liquefaction induced downdrag for the Juan Pablo II Bridge at the 2010 Maule earthquake in Chile. Geotechnical Engineering Journal of the SEAGS & AGSSEA, June 2020, 51(2) 1-18.

Liquefaction Induced Downdrag for the Juan Pablo II Bridge at the 2010 Maule Earthquake in Chile

Bengt H. Fellenius[1], Babak Abbasi[2], and Balasingam Muhunthan[3]
[1]*Consulting Engineer, Sidney, BC, Canada*
[2,3]*Department of Civil and Environmental Engineering, Washington State University, USA.*
[1]E-mail: *bengt@fellenius.net*
[2]E-mail: *babak.abbasi@wsu.edu*
[3]E-mail: *muhuntha@wsu.edu*

ABSTRACT: Sandy soil layers reduce volume during and following liquefaction, which results in settlement of the overlying soil layers. In case of pile constructed in the liquefying soil, the liquefaction-induced settlement induces downward directed shear stress (negative skin friction) along the pile causing the pile to settle—be dragged down. Depending on the site conditions, the change in the axial response resulting from liquefaction-induced settlement, and downdrag can have a significant impact on piled foundation performance in seismic regions. This study presents an analytical method to quantify the effects of liquefaction-induced downdrag on drilled shafts. The method relies on combining two diagrams. One diagram shows the distributions of force along the pile in negative and positive direction displaying a force equilibrium. The other diagram shows the distribution of soil and pile movement, displaying a settlement equilibrium. The analysis method consists of combining the force movement of the pile and the soil so that the two equilibriums occur at the same depth, called the "neutral plane". The method, called the "unified analysis method", is applied to an observed case of downdrag during the February 7, 2010, Maule Magnitude 8.8 earthquake in Chile showing that the calculated settlements are close to those observed at the site. The results of the unified analysis indicate that the major effect on the pile settlement was from liquefaction-induced settlement below the pile toe level, as opposed to downdrag. The case study shows the importance of combining forces and movements in the analysis of piled foundation settlement.

KEYWORDS: Piled foundations, Liquefaction, Downdrag, Negative skin friction, Settlement analysis.

1. INTRODUCTION

Deep foundations are generally used to transfer structural loads to deeper strata. The loads may be axial, lateral, or a combination of both. Load transfer from shaft to soil ,or vice versa, includes a relative movement between shaft and soil, which mobilizes shaft and toe resistances.

Sandy soil layers reduce volume during and following liquefaction (Tokimatsu and Seed 1987, Ishihara and Yoshimine 1992). The volume reduction appears as a downward movement—settlement—of the overlying soil layers. The downward movement of the soil relative the pile induces shear stress along the shaft commonly called "negative skin friction". The accumulated negative skin friction will add axial force to the pile, called "drag force".

In seismic regions, depending on the site conditions, the change in axial response resulting from liquefaction-induced settlement can have a significant influence on the pile. In extreme circumstances, the drag force plus sustained load from the structure may exceed the structural axial strength of the pile for very long piles (aspect ratio larger than about 100). The soil settlement around the pile will tend to move the pile downward, i.e., add downdrag, that may affect the serviceability of the structure. Incidences of liquefaction-induced downdrag of apparently excessive amounts occurred at the February 7, 2010, Maule Magnitude 8.8, earthquake in Chile (Yen et al. 2011).

Unlike the case of development in consolidating soils, only a few analytical studies have addressed drag force and downdrag where the soil settlement is caused by seismic liquefaction, (Boulanger and Brandenberg 2004, Rollins and Strand 2006, and Fellenius and Siegel 2008). Boulanger and Brandenberg (2004) related the shaft resistance in a reconsolidating liquefied zone to the dissipation of excess pore pressure over time and estimated the resulting drag force. Downdrag developed incrementally over time in parallel with the pore pressure dissipation.

Methods to account for effect of liquefaction on deep foundations are addressed in terms of drag force development in a few design manuals, such as AASHTO (2014) and WSDOT (2013). The AASHTO (2014) specifications for piled foundation design recommend adding the factored drag force from the soil layers above the liquefiable zone to the factored loads from the superstructure and requiring the sum to be smaller than the factored shaft and toe resistances below the zone. Fellenius and Siegel (2008) questioned the validity of the AASHTO Specifications in case of liquefaction-induced downdrag.

Fellenius and Siegel (2008) applied the unified method (Fellenius 1984; 2004; 2020) to pile analysis to account for seismic liquefaction effects. The Unified Method is based on the concept of force and settlement equilibriums in the pile develop at the same depth, called the neutral plane (NP) and accounts for the interaction between pile resistance and soil settlement, the most decisive being the interaction between toe resistance and toe penetration.

Fellenius and Siegel considered the location of a single liquefiable zone with respect to whether the liquefiable zone is located above or below the NP. The validity of the approach has been demonstrated for a case in northern California (Knutson. and Siegel 2006) and for field tests (Rollins and Strand 2006 and Strand 2008). This method is here applied to the case of the performance of the bores pile foundation supporting the Juan Pablo II Bridge that failed during the Maule Chile Earthquake in 2010.

2. THE FEBRUARY 7, 2010 EARTHQUAKE IN CHILE

On February 7, 2010, a magnitude 8.8 earthquake struck in the Pacific Ocean just outside Chile. The earthquake epicenter was located approximately 330 km (200 miles southwest of Santiago, 100 km (65 miles) northeast of Concepción, and 110 km (71 miles) west-southwest of Talca. The depth of the earthquake hypocenter was 35 km (22 miles). The earthquake was characterized by its long duration (>2 minutes) and strong ground motion. Recorded peak ground accelerations at Station Colegio San Pedro, Concepción (CCSP), in the directions of NS, EW, and vertical were 0.65g, 0.6 g, and 0.58g, respectively (Yen et al. 2011). It caused surface deformation, structural damage, and loss of life. The transportation network, including roads, embankments, and bridges were affected.

Geotechnical failures consisted of landslides, uplifts, and widespread liquefaction, especially along the coastline and rivers. Nearly 200 bridges suffered varying degrees of damage to both superstructures and foundations. Many of these bridges were designed after the mid-1950s in accordance with the then AASHTO

Standard Specifications for Highway Bridge Design (Yen et al. 2011).

The Juan Pablo II Bridge is the longest vehicular bridge in Chile, and it connects the cities of Concepción and San Pedro de la Paz by traversing the Bío-Bío River in the NE-SW direction as shown in Figure 1. It was opened to the public in 1974 and it is nearly 2 km long, with more than 70 spans of 22 m wide, 33m long concrete decks, each span having seven reinforced concrete girders. The span supports are reinforced concrete piers founded on two 2.5 m diameter and approximately 16 m long piles (Ledezma et al. 2012).

The Juan Pablo II Bridge piers settled substantially at various locations and the bridge had to be closed to public access. Verdugo and Peters (2010) reported settlements of about 200, 400, 450, and 650 mm (7.9, 15.7, 17.7, and 25.6 in), respectively, of Piers 1-2 and 5-6 at the approach toward Concepción, and Support Piers 117-118 and 119-120 at the approach toward San Pedro. The locations of these piers are indicated in Figure 1.

Figure 1 Google Earth view of Juan Pablo II Bridge

A report by the GEER (2010) documented that the northeast approach (toward Concepción) of the bridge suffered more damage and settlement than the southwest approach (toward San Pedro). For the study reported herein, the records of Piers 1-2 (BH-16) and 5-6 (BH-10), toward the southwest end of the bridge and Piers 117-118 (BH-3) and 119-120 (BH-7), toward the northeast were selected. Figure 2 shows a plan view of the support pier locations and closest boreholes.

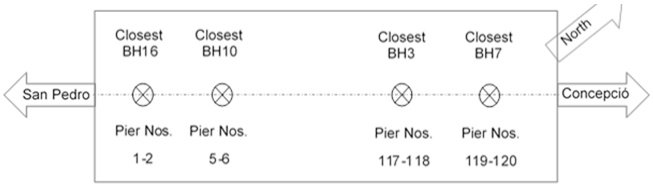

Figure 2 Schematic diagram for piers and nearby boreholes along Juan Pablo II Bridge

Figure 3 shows the distribution of grain sizes, soil types, water content, and N-indices at BH-3. The N-index diagram delineates the potentially liquefiable zones at the borehole as determined using the Youd et al. (2001) procedure. Three potentially liquefiable zones are indicated within the pier embedded lengths. The first zone is at the ground surface and is about 3 m thick. Second and third such zones are 0.9 and 4.0 m thick and located between the depths of 7 through 8 m and 9 and 13 m depth, respectively. In BH-3, an about 0.9 m thick liquefiable zone is identified closely below the pile toe. Three additional, about 2 to 8 m thick zones exist below the pile toe starting at depths of about 24, 32, and 33 m depth. Thickness and location of the liquefiable zones likely vary between the boreholes.

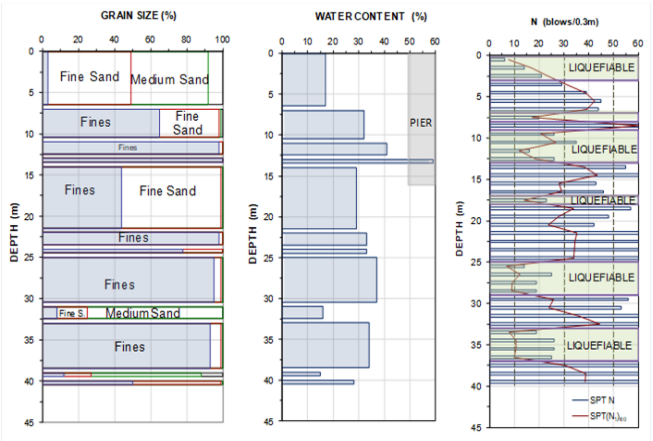

Figure 3 Borehole 3: Grain size, water content, N-indices—measured and adjusted to (N60.

SPT N-index correction factors, such as correction for borehole diameter (CB), correction for sampler type (CS), correction for rod length (CR), and correction for hammer energy ratio (CE) are assumed to be 1.05, 1.0, 0.85, and 0.85, respectively; and the maximum overburden correction factor (CN) is 1.7. Fine content variation with depth and normalized SPT N-values, (N1)60, were applied to determine the liquefiable zone identified in the figures. Additional liquefaction susceptibility parameters, such as cyclic stress ratio (CSR), ratio of total stress to effective stress (σv/σv'), and stress reduction coefficient (rd) ranged from CSR of 0.4 to σv/σv' of 0.9, 2.0 to 2.2, and rd of 0.4t to 1.0, respectively. Values of (N1)60 below 30 blows/0.3m (boundary between compact and dense conditions) were considered representative for a liquefiable zone as indicated in Figure 3. Although the method supposedly only applies to depths above 25 m it has been used to delineate the liquefiable zones also below this depth.

Tokimatsu and Seed (1987) proposed a correlation for post-liquefaction volumetric compressions of liquefiable zones. The procedure comprises estimating the volumetric strains from correlation to (N1)60 and cyclic stress ratio (CSR) via a family of curves. The post-liquefaction settlement is calculated by integrating volumetric strain over the thickness of each liquefiable zone. Each liquefiable zone was divided into sub-zones with constant SPT N-index. The cumulative post-liquefaction settlement was obtained by adding the settlement of the individual zones. Figure 4 shows the distribution of post-liquefaction settlement calculated at the four borehole locations. The family of curves proposed by Tokimatsu and Seed (1987) is inserted in the figure. It is interesting to note that the method indicates that more than half of the calculated settlement would occur below the pier toe level of the piles supporting Pier 117.

3. ANALYSIS PROCEDURE

3.1 Shaft and Toe Resistances

The first step in n analysis of a pile is to compile all pertinent soil and pile information and the short and long-term loads and soil movements affecting the pile. The next is to determine the shaft resistance distribution and the pile toe response. The shaft resistance portion of the force distribution curves assumes that a more than a small relative movement, typically about 5 mm, more or less, has been mobilized. It is usually acceptable to assume a that the shaft resistance beyond this value is independent of additional movement between the pile and the soil, which is akin to assume an ultimate unit shaft resistance. It also disregards the fact that shaft resistance is usually either strain-hardening or strain-softening, which is not always the case, but considered applicable for sand.

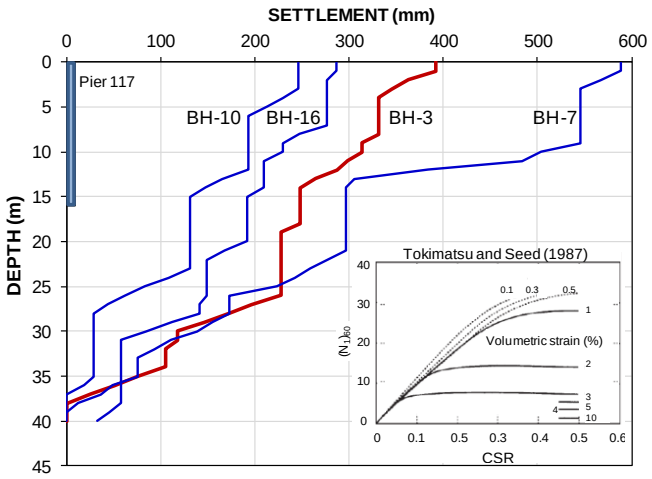

Figure 4 Post-liquefaction soil settlement profile near BHs 3, 7, 10, and 16 using the Tokimatsu and Seed (1987) procedure (after Vijayaruban, 2014)

Conventionally, an ultimate shaft resistance distribution is obtained by back-calculation of results from static loading tests (when available). It is generally recognized that the shaft resistance is proportional to effective overburden stress expressed by a proportionality coefficient, a ß coefficient. In the absence of test and local experience, the distribution is estimated from in-situ tests (cone penetrometer, CPTU, and SPT borehole with N indices).In regard to toe resistance, however, the movement associated with the mobilization of the toe resistance cannot be disregarded. The typical pile-toe force-movement response follows a exponentially decaying curve that usually can be expressed by a power function shown in Eq. 1 (Gwizdala 1996, Fellenius 2020).

$$\frac{R_1}{R_2} = \left(\frac{\delta_1}{\delta_2}\right)^{\theta} \qquad (1)$$

where R_1 and R_2 = any of two resistances

δ_1 and δ_2 = movements mobilized at R_1 and R_2, respectively

θ = function coefficient; an exponent ranging from a small value through unity. Typical toe coefficients for sand range from 0.5 to 0.8.

To illustrate the typical pile-toe response, Figure 5 shows records of pile-toe force vs. movement measured at static loading tests on three piles. One was performed on a 1,200 mm diameter, 23 m long bored pile constructed though sandy silt into a dense silty sand (Fellenius and Tan 2012). The second is from a 400-mm diameter 42 m long, bored pile constructed through loose sand to bearing in dense sand. The third is from a 300 mm diameter, 18 m long, precast concrete pile driven into a loose uniform sand (Fellenius 1970, Tavenas 1971).

The test data have been normalized to show stress versus pile-toe movement in percent of the pile diameter. Gwizdala function coefficients of 0.64 and 0.50 gave calculated curves with a good fit to the respective records of the bored piles. For the third pile, as is typical for a driven pile, the toe-force vs. movement curve of the driving pile rose steeply at first, and more gently later. The initial steep rise is an indication of residual force (locked-in force) in the pile, prestressing the soil below the pile toe. A fit using a Gwizdala function suggested a function coefficient of 0.23, which does not provide a good for either the beginning or the end of the curve. Using a hyperbolic function (Chin) provided a better fit to the test data. However, a hyperbolic function implies that the toe resistance would trend to an ultimate value, which is not correct for toe resistance. A bored pile of the same size, at the same location, and the same depth would probably have show a force-movement curve for the pile toe similar to the driven pile curve after adjustment for residual load. However, for estimating a toe resistance from a toe movement or vice versa in regard to the case record, either of the two fitted function curves, Gwizdala and Chin, fit would be suitable.

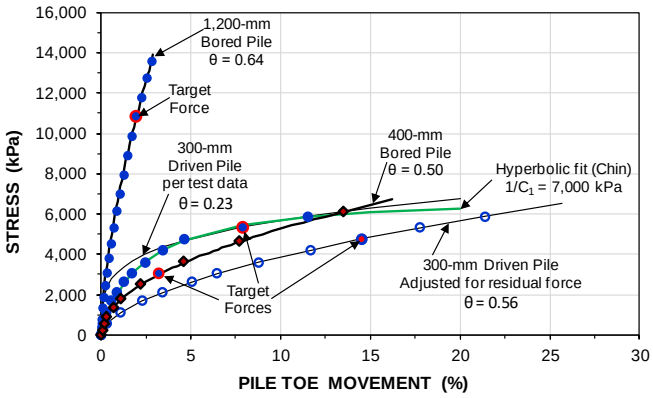

Figure 5 Toe resistance versus toe movement curves for two test piles and simulation of the measured curves using a Gwizdala q-z function.

It is obvious that no specific toe resistance value would meaningful unless associated with its movement. Yet, in current practice, a toe resistance is often quoted without an associated movement value. It is often assumed that an "ultimate toe resistance" occurs at a distance equal to 5 % of the pile toe diameter. That value is no more relevant than the sometimes proposed definition of pile capacity—ultimate shaft and toe resistances, together—as being 10 % of the pile diameter. Indeed, the three test records could have been plotted to show stress normalized to an assumed ultimate value and the pile toe movements normalized to percent of the movement for that resistance. However, other than obtaining a plot showing curves having a common point at 100% stress/100% movement, and diverging before and after, nothing else particular would have been learnt.

3.2 Distribution of loads and settlement in the long-term

Two different thoughts have been proposed for the long-term, before-liquefaction condition. The first (Alt. I) assumes that no drag force and downdrag has developed before a liquefaction event especially in sandy soils (AASHTO 2014) and the other (Alt. II) assumes that due to creep and other phenomena that introduces settlement in the soil body, drag force and downdrag will have developed before the liquefaction event.

The unified method (Fellenius 1984; 2004; 2020) recognizes both alternatives. As to Alt. II, after completion of construction of

piled foundations and supported structure, the soil will settle in relation to the piles and the axial load in the piles will increase until a steady state has been reached. The process can take a long time or be short. The unified method establishes the long-term condition by determining four distribution curves that will develop after the completed construction.

1) a load curve showing the distribution of force consisting of the sustained (dead) load applied to the pile head increasing by accumulated shaft resistance in negative direction,
2) a resistance curve showing the distribution force starting from an assumed pile toe resistance and increasing upward by accumulated shaft resistance, intersecting and joining the load distribution curve,
3) the distribution of soil settlement, and
4) the distribution of pile movement starting from an assumed pile toe movement and proceeding upward with the increase due to the axial force in the pile, which are easily estimated—the curve is essentially a line sloping slightly to the side—intersecting the settlement distribution.

Figure 6 shows the four distribution curves of the unified method for the 400-mm diameter bored pile used in Figure 5 to illustrate pile toe response. The soil settlement will be the consequence of a future 2-m lowering of the groundwater table due to water mining in the area and consolidation of placing a 1.5 m thick fill across the general site.

A CPTU graph is also added to the figure showing the distribution of the CPTU cone stress, q_t. The loose sand layer between 16 and 40 m depths is estimated to experience liquefaction at some depths in the event of an earthquake.

The load and resistance curves intersect where the loads above is equal to the resistance below. The intersection occurs where shaft shear has changed from negative to positive direction and it is called "force equilibrium". Assuming that the unit shaft resistance is independent of the magnitude of the movement between pile and soil, then, the depth to the intersection depends entirely on the magnitude of the assumed toe resistance. N.B., an assumed pile-toe resistance decides the pile-toe movement and vice versa.

Also the soil settlement curve and the pile movement curve will intersect. The depth to the intersection depends primarily on the value of toe resistance considered in the analysis, which is a function of the pile toe movement. The intersection between defines the depth where the pile and the soil move equally. That is, above the intersection, the soil moves more and negative skin friction develops. Below, the pile moves more an the positive shaft resistance develops. The intersection is called "settlement equilibrium" and, obviously, it must occur at the same depth as the "force equilibrium".

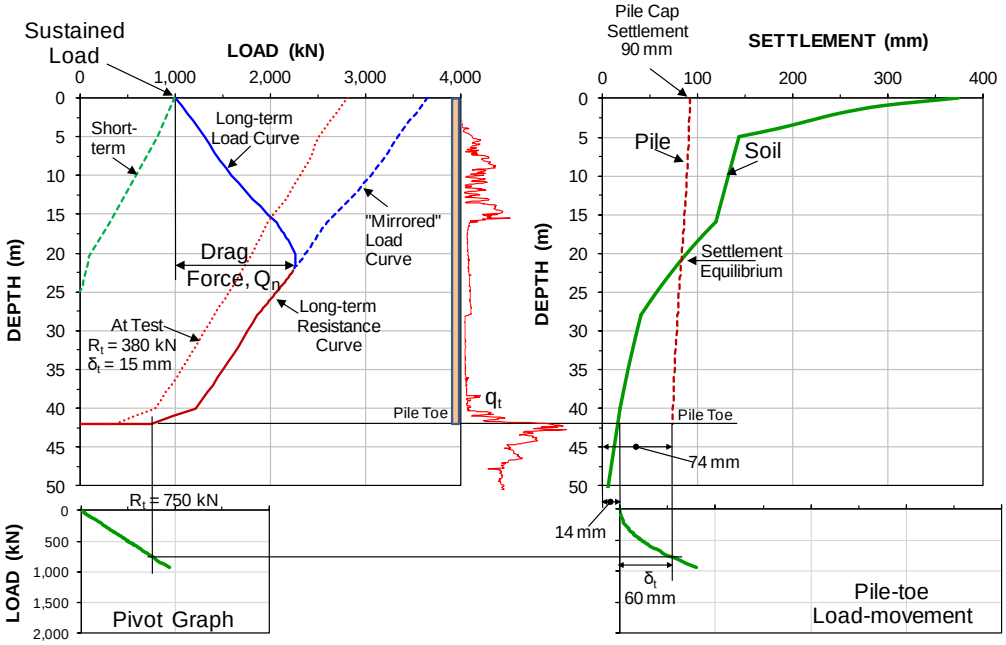

Figure 6 Long-term distributions of load and resistance for a single pile

The load distribution curve and the resistance distribution curve are plotted in load-resistance diagram and the soil settlement distribution and pile movement together in a settlement diagram. The load and resistance distribution diagram is supplemented with the "short-term" load distribution—the distribution immediately after completed construction for the working load applied to the pile (as determined in a static loading test performed the piles; it was a strain-gage instrumented test pile). This curve represents the Alt. I condition.

A graph showing the pile-toe load-movement response is added below the settlement-distribution diagram and the "pivot diagram" below the load-distribution diagram shows how the toe force and toe movement connect between the two main plots. Any chosen pile toe resistance and pile-toe movement make up a pair that must agree with the pile toe load-movement relations—measured, calculated from soil input, or estimated from a q-z function, usually per a Gwizdala function.

At first try, the two equilibriums will not be found at the same depth. To move them closer to being at the same depth, the assumed toe resistance needs to be adjusted up or down—per judgment—which changes the depth of the force equilibrium. Because the assumed toe movement will have to be adjusted to fit the toe-force response in accordance with the particular q-z relation, also the depth to the settlement equilibrium will change. After a couple of such adjustments, the two equilibriums will be found to occur at the same depth, now called the "neutral plane".

The force equilibrium is where the maximum axial load will develop (c.f., Figure 6). The difference between the working load and the maximum load is called "drag force" and it is a passive force of concern only for the pile structural strength, which might be the case for a long pile.

3.3 Distribution of loads and settlement

In the short-term, Alt. I, no negative skin friction acts along the pile. Only positive shaft resistance exists as mobilized to the extent needed for the soil to carry the applied load. If liquefaction occurs somewhere along the pile, then, the shaft resistance will reduce or become zero in the liquefied zone and the axial resistance previously obtained within that zone will be demanded from the soil layers below. In the process, the pile compression will increase and, if the shaft resistance below the liquefied layer or zone is insufficient to meet the increased demand, then, the pile toe will and, to do so, it will move down, corresponding to the applicable q-z relation. This will result in a piled foundation settlement as a sum of the pile-toe movement and the increased compression of the pile. After the liquefaction, when consolidation develops as the induced pore pressures dissipate, soil layers above the liquefied zone will settle—a rapidly occurring condition—and the load and resistance distribution in the pile will resemble something in-between the short- and long-term distributions of Figure 6. The movement of the pile and, therefore, the settlement of the piled foundation will be governed by the pile toe movement..

If an earthquake occurs very early in the life of a structure, then, Alt. I can be real. However, in the long-term, even if there is no consolidation or increased loading of the soil, aging effect will make the soil move down in relation to the pile—already very small movement will have this effect. Although, in case of very small relative movements, the height of the transition zone will be large (the transition zone is where negative direction of shear of the load distribution curve changes to positive direction of shear of the resistance distribution).

Alt. II illustrates the long-term case (Figure 6) when negative skin friction has occurred and a neutral plane developed. If an earthquake occurs triggering liquefaction throughout the 25-m layer of loose sand, the piles might survive, but the structure might not and, if the structure is a building with occupants, they might not either. The geotechnically interesting case is where the liquefied zone is limited in thickness and, more specifically, if the liquefied zone lies above or below the neutral plane, and in the latter event, if that zone lies above or below the pile toe level.

Figure 7 shows the effect before and during liquefaction occurring in a zone of limited thickness located above the neutral plane. The liquefaction will cause the shaft resistance to reduce or become zero within the liquefied zone. When zero shaft resistance, the only increase of axial force in the pile would be from the buoyant weight of the pile within that zone—a negligible amount. This will result in a reduction of the load in the pile, a small release of axial compression, and, theoretically, a corresponding heave of the pile head, though the constraining effect of the pile cap would prevent this. After dissipation of the pore pressures induced in the liquefied zone, the load and resistance distribution will return to the original shape and as there would have been no change in toe conditions, there will be no foundation settlement.

Figure 8 shows the response if the load and resistance distribution curves and soil and pile settlement for the case of the liquefaction occur in a zone located below the neutral plane. The reduction of shaft resistance in the liquefied zone would cause an immediate transfer of load to the pile toe and a settlement of the pile caused by the pile-toe movement (due to the increase of the pile-toe force). The subsequent consolidation of the liquefied zone resulting from the pore pressure dissipation will add to the liquefaction-caused settlement of the soil. The total settlement of the pile cap, the downdrag, will be due to increased axial compression (because the force equilibrium will have moved down in response to the increased toe resistance and the increased pile toe movement due top the downdrag—its magnitude will be determined by the toe stiffness, the q-z relation. The axial compression will not likely be significant, but depending of the pile-toe response, the pile toe movement could be substantial, as would also the foundation settlement.

If the liquefaction would occur just below the pile toe level, then, the toe resistance would reduce or become zero and the pile would move down until the working load becomes carried by shaft resistance along its full length. If the shaft resistance would be smaller than the working load, the pile would plunge and the foundation would fail. If the liquefaction would occur well below the pile toe level, the effect would be a settlement of the pile-soil body corresponding to the compression (loss of volume) of the liquefied zone, but no effect on in regard to shaft and toe resistances.

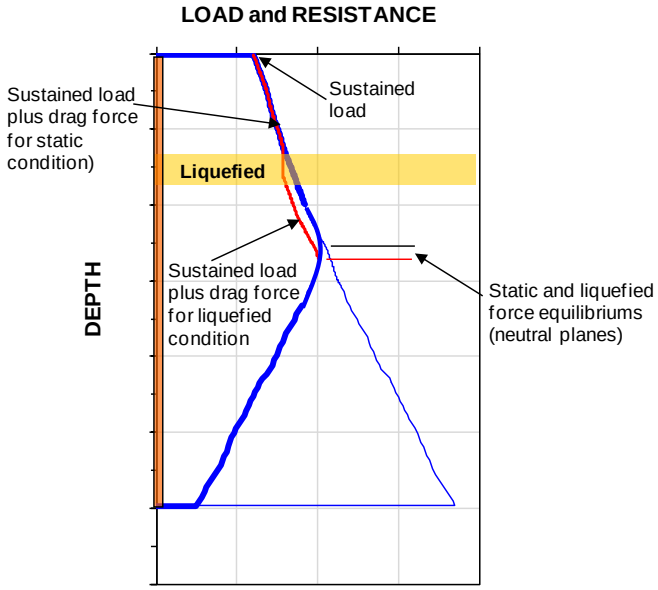

Figure 7 Effect of liquefaction above the force equilibrium neutral plane

4. ANALYSIS OF THE PILES SUPPORTING PIER 117 OF THE JUAN PABLO BRIDGE

Pier 117 was supported on two bored piles that extended above the ground to a pile-bent beam. The pile had 1.5 m diameter and was 16 m long. The average sustained load per pier is estimated to have been 12,700 kN , which is calculated based on weight of bridge span, girder, wearing surface, and column applying 24 kN/m^3 and 75 kN/m^3 as unit weights of concrete and steel, respectively.

The distribution of effective overburden stress at the site is determined from the groundwater table located near the ground surface, hydrostatic pore pressure distribution, and soil density determined from the water content values shown in Figure 2. However, no static loading test was carried out and the only information for use in estimating the pile response to the applied load consists of the borehole soil description and SPT N-indices (c.f., Figure 3). The unit shaft resistance is linearly proportional to the effective overburden stress by a proportionality coefficient termed ß-coefficient. Meyerhof (1976), Decourt (1989), and O'Neill and Reese (1999) proposed relations showing ß as a function of the N-index. The O'Neill and Reese relation is also included in ASAHTO (2014). However, it is not applicable to soils with where N > 15 blows/0.3m. Figure 9 shows the distribution of ß-coefficients calculated using the Meyerhof and Decourt method for the records of BH-3. Also shown is the ß-distribution assigned to the analysis of the shaft resistance at Pier 117.

A toe resistance can be estimated from the N-indices. However, the various relations proposed in the literature produce a single ultimate resistance without including the associated toe penetration. The result is therefore rather dubious. A q-z relation is necessary, as indicated in the foregoing (Eq. 1 and Figure 5). For a very dense sand indicated for the soil layers below the pile toe level (apart from the liquefiable zones), it is reasonable to assume that the pile response would be a load-movement curve according to the Gwizdala function with θ equal to 0.6. The ß coefficient distribution indicated from the N-indices in BH-3 amounts to a fully mobilized, total shaft

resistance of 5,240 kN, which can be assumed to be mobilized after an about 5 mm relative movement. Moreover, the shaft resistance in the compact to dense sand at the site can be assumed to be neither strain-hardening nor strain-softening for further movement.

event. However, as put forward by Fellenius and Siegel (2008), also in sand, in the long-term, there will be a small settlement of the soil around the pile, developing a force equilibrium in the pile and an

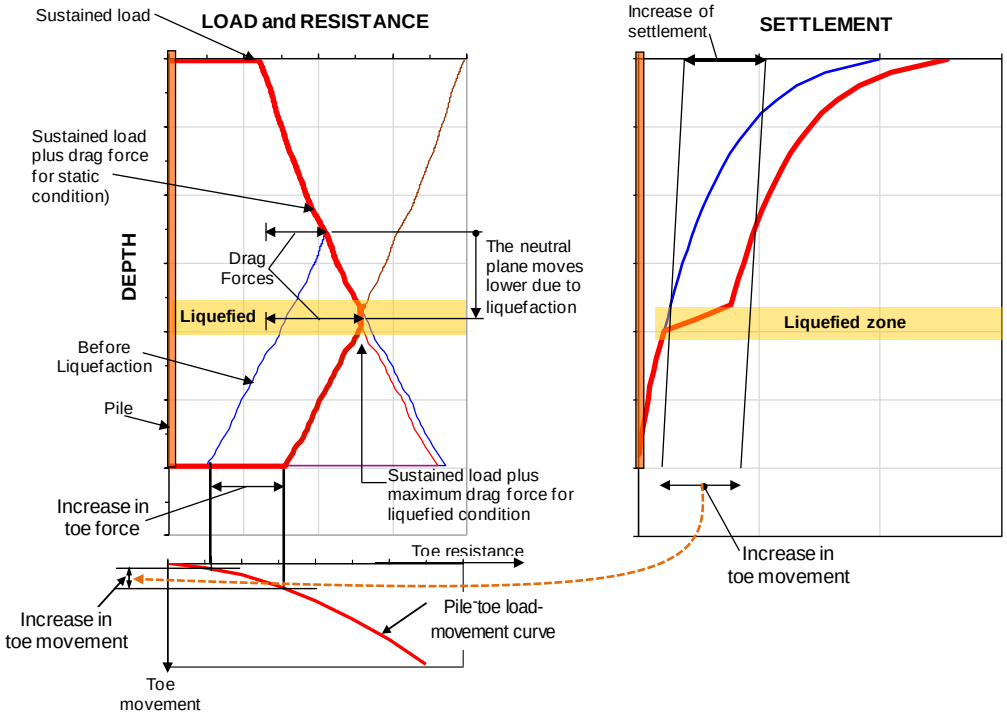

Figure 8 Effect of liquefaction occurring below the force-equilibrium neutral-plane.

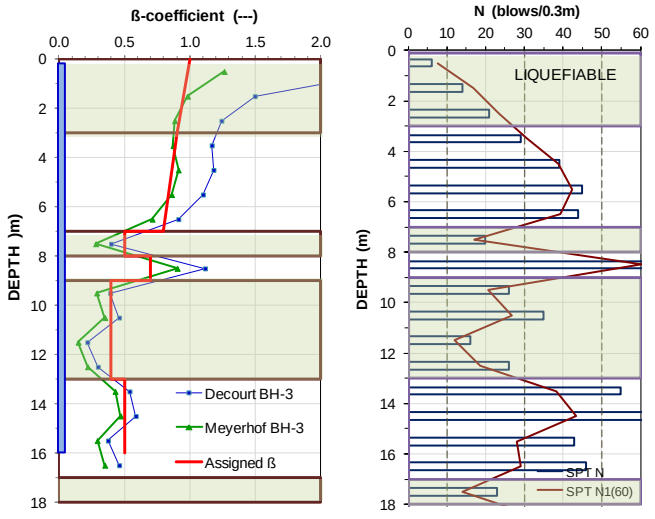

Figure 9 Distribution ß-coefficients from N-indices in BH-3 and assigned distribution

The balance of the 12,700-kN sustained load, 7,450 kN (1,500 kPa toe stress) can be assumed to cause a pile toe movement of about 10 to 12 mm, that is, a movement larger than the about 5 mm assumed to cause full mobilization of the shaft resistance. For the analysis, it was assumed that a 6,000-kN toe force would result in a 8-mm pile-toe movement. Applying θ = 0.6 , the toe-resistance relation becomes Rt = 1,700·δt0.6 (4.1·10^-6·δt = Rt3/5) with force units in kN and movement units in mm. Thus, the 7,450-kN toe force would result in a 11.6-mm toe movement.

The 5,300 kN shaft resistance and 7,400 kN toe force act on completed construction. Alt. I, mentioned above, indicates this to be also the long-term distribution, i.e., at the onset of the liquefaction

increase of pile toe force and is right at the pile toe, which would result in a pile toe force of 18,000 kN (the sustained load plus fully mobilized drag force) and be associated with a 50 mm toe movement. However, it is more likely that a force equilibrium would develop well above the pile toe and result in a smaller toe force, somewhere between the 7,400-kN post construction value and the 18,000 kN maximum, say, at 12,500 kN, which would be associated with an about 25 mm toe movement and a force equilibrium located at 9.0 m depth. The height of the transition zone between negative direction shear forces to positive direction was estimated to be about 4 m (about 1.5 pile diameter). This is what was termed Alt. II. The drag force will have been minimal.

At post-equilibrium, the soil settling around the pile will cause the soil settling around the piles and negative skin friction will develop around the full length of the pile. The downdrag will amount to the mentioned 50-mm pile toe movement less the long-term movement present before the liquefaction event, i.e., 11 mm and 25 mm, respectively, c.f., Table 1. No transition zone is expected to have developed.

Table 1 Pile-toe forces and pile-toe movements

Event	R_t (kN)	δ_t (mm)
Post-construction (and Alt. I)	7,450	12
Long-term	12,500	25
Post-liquefaction	18,000	50

R_t = toe force and δ_t = toe movement

Figure 10 presents the three load distributions: on completed construction (also Alt. I), long-term condition (also Alt. II), and post-liquefaction condition. The figure includes a diagram showing the distribution of soil settlement determined from the N-indices of BH 3 (c.f., Figure 4) and the pile -toe load-movement curve below the settlement diagram). The pivot-graph below the load-distribution graph connects the pile toe forces to the associated pile-toe movements. All calculations were performed using the UniPile5 software (Goudreault and Fellenius 2014).

the Tokimatsu and Seed method and the values are similar to the those observed at the bridge site.

An effective stress analysis was used to determine the distribution of shaft resistance and magnitude of toe resistance associated with the pile-toe movements. The pile toe forces and pile-toe movements at post-construction, long-term conditions, and post-liquefaction were estimated and showed that before the liquefaction event the pile-head settlement was about 10 to 25 mm.

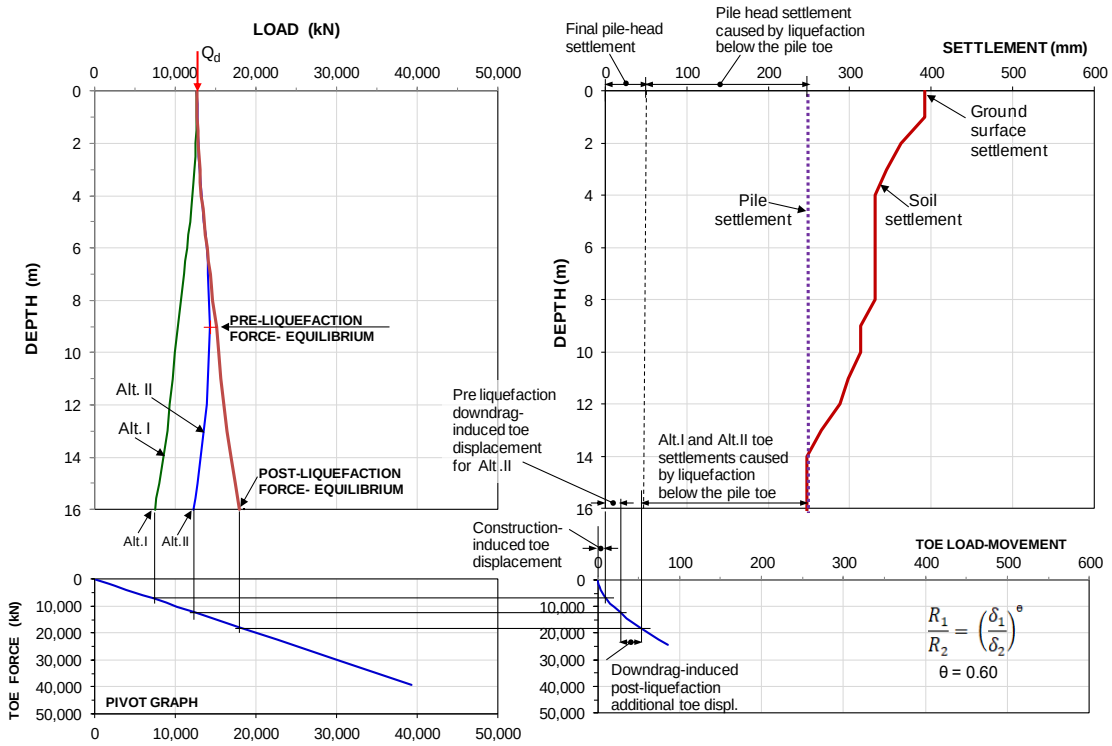

Figure 10 Effect of liquefaction occurring below the force-equilibrium neutral-plane.

Of course, with different input regarding the ß-coefficient and the q-z curve, the calculated forces and pile movements would differ from the here presented. However, the calculated maximum post-liquefaction, pile-head movement now close to 50 mm would not have been much larger (nor smaller). Thus, as is indicated in Figure 10, the largest portion of the foundation settlement was caused by liquefaction at depth below the pile toe level. and not by downdrag. Moreover, the magnitude of the drag force has been inconsequential for the pile and its response to the liquefaction.

Ordinarily, the weight of the pile analyzed is not considered in the analysis of the pile response. However, for the subject rather large diameter pile in respect to the pile length, 2.5 m and 16 m, respectively, the pile weight does have a noticeable effect. The buoyant weight was about 70 kN/m and the total weight was about 1,000 kN, increasing the pile toe force correspondingly. It can be included in the analysis by correspondingly decreasing the ß-coefficient, when analyzing the load distribution and similarly increasing it to the same degree when calculating the resistance distribution. Including the pile weight would have added about 5 mm to the calculated of toe movements, which would not have mattered much in comparing the downdrag to the settlements below pile toe.

5. CONCLUSIONS

This study presents an analytical method to quantify the effects of liquefaction-induced settlement of the piled foundation of the Juan Pablo bridge at Juan Pablo II Bridge at the 2010 M8.8 magnitude Maule earthquake in Chile.

The settlements due to the liquefaction were estimated applying

The liquefaction caused the soil to settle around the piles and resulted in an additional settlement due to downdrag of about 40 to 25 mm. The liquefaction below the pile toe level induced a foundation settlement several times larger and was the main cause of the failure of the bridge foundations.

6. ACKNOWLEDGEMENTS

Support for this work was provided by Washington State Department of Transportation is acknowledged under grant to Washington State University.

7. REFERENCES

American Association of State Highway and Transportation Officials, 2014. *LRFD Bridge Design Specifications*, seventh edition, 2014, U.S. customary units : 2015 interim revisions.

Boulanger, R.W., and Brandenberg, S.J., 2004. Neutral Plane Solution for Liquefaction-Induced Down-Drag on Vertical Pile. In *Proc. of Geot. Engnng for Transportation Projects*. Geo-Trans 2004, Los Angeles, July 27-31, pp. 470-478.

Decourt, L., 1989. The Standard Penetration Test. State-of-the-Art report. A.A. Balkema, Proc. of 12th International Conference on Soil Mechanics and Foundation Engineering, Rio de Janiero, Brazil, August 13-18, Vol. 4, pp. 2405-2416.

Fellenius, B.H., 1970. Friktionspålars bärförmåga—Resultat av fältförsök. Royal Swedish Academy of Engineering Sciences, Commission on Pile Research, Report No. 22, 24 p. (In Swedish).

Fellenius, B.H., 1984. Negative Skin Friction and Settlement of Piles. In *Second International Seminar, Pile Foundations*. Nanyang Technological Institute, Singapore, 18p.

Fellenius, B.H., 2004. Unified design of piled foundations with emphasis on settlement analysis. Honoring George G. Goble—Current Practice and Future Trends in Deep Foundations. Geo-Institute Geo-TRANS Conference, Los Angeles, July 27-30, 2004, Edited by J.A. DiMaggio and M.H. Hussein. ASCE Geotechnical Special Publication, GSP125, pp. 253-275.

Fellenius, B.H., 2020. Basics of foundation design—a textbook. Electronic Edition, www.Fellenius.net, 524 p.

Fellenius, B.H. and Siegel, T.C., 2008. Pile Drag Load and Downdrag in a Liquefaction Event. *Journal of Geotechnical and Geoenvironmental Engineering*, 134(9) 1412–1416.

Fellenius, B.H. and Tan, S.A., 2012. Analysis of bidirectional-cell tests for Icon Condominiums, Singapore. In *Proc. of the 9th Int. Conf. on Testing and Design Methods for Deep Foundations*, Kanazawa, Japan, Sept. 18-20, 2012. 10 p.

FHWA, 2010. Drilled Shafts: Construction Procedures and LRFD Design Methods. *Handbook*, (132014), 972 p.

Goudreault, P.A. and Fellenius, B.H., 2014. UniPile Version 5, User and Examples Manual. UniSoft Geotechnical Solutions Ltd. [www.UniSoftGS.com]. 120 p.

Gwizdala, K., 1996. The analysis of pile settlement employing load-transfer functions (in Polish). Zeszyty Naukowe No. 532, Budownictwo Wodne No.41, Technical University of Gdansk, Poland, 192 p.

Ishihara, K. and Yoshimine, M., 1992. Evaluation of Settlements in Sand Deposits Following Liquefaction during Earthquakes. *Soils and Foundations*, 32(1) 173–188.

Knutson, L. and Siegel, T.C., 2006. Consideration of Drilled Displacement Piles for Liquefaction Mitigation. In *Proc., DFI Augered Cast-In-Place Pile Committee Specialty Seminar*. pp. 129-132.

Ledezma, C., Hutchinson, T., Ashford, S. A., Moss, R., Arduino, P., Bray, J. D., Olson, S., Hashash, Y. M. A., Verdugo, R., Frost, D., Kayen, R., and Rollins, K. (2012). Effects of Ground Failure on Bridges, Roads, and Railroads. *Earthquake Spectra*, Earthquake Engineering Research Institute , 28(S1), S119–S143.

Meyerhof, G.G., 1976. Bearing capacity and settlement of pile foundations. The Eleventh Terzaghi Lecture, November 5, 1975. ASCE Journal of Geotechnical Engineering 102(GT3) 195 228.O'Neill, M.W. and Reese, L.C., 1999. *Drilled Shafts. Construction Procedures and Design Methods* FHWA-IF99-ed. Transportation Research Board, ed., Federal Highway Administration, Washington, 790 p.

O'Neill, M.W. and Reese, L.C., 1999. Drilled shafts. Construction procedures and design methods, Federal Highway Administration, Transportation Research Board, Washington, FHWA-IF99-025.

Rollins, K. and Strand, S., 2006. Downdrag Forces Due to Liquefaction Surrounding Piles. In *8th U.S. National Conference on Earthquake Engineering*. San Franciso, Paper No. 1646, 10 p.

Strand, S.R., 2008. *Liquefaction Mitigation Using Vertical Composite Drains and Liquefaction-Induced Downdrag on Pile : Implication for Deep Foundation Design*. Brigham Young University, Salt Lake City, UT, Ph.D. Thesis.

Tavenas, F.A., 1971. Load tests results om friction piles in sand. Canadian Geotechnical Journal, 8(7) 7-22.

Tokimatsu, K. and Seed, H.B., 1987. Evaluation of settlements in sands due to earthquake shaking. *Journal of Geotechnical Engineering*, 113(8) 861–878.

Verdugo, R., Peters, G., 2010. Informe Geotécnico Fase Anteproyecto Infraestructura Puente. *Mecano Eje Chacabuco*, (Rev7).

WSDOT, 2013. *Washington State Department of Transportation* M 46-03.09., Geotechnical Design Manual.868 p.

Vijayaruban, N.V., 2016. *Liquefaction-induced downdrag on piles and drilled shafts*. Washington State University, Pullman, WA, Ph.D. Thesis.

Yen, W.-H.P. et al., 2011. *Post-Earthquake Reconnaissance Report on Transportation Infrastructure: Impact of the February 27, 2010, Offshore Maule Earthquake in Chile, 214 p.*